


## Article

# Study on the Correlation Between Mechanical Properties, Water Absorption, and Bulk Density of PVA Fiber-Reinforced Cement Matrix Composites

Wen Xu <sup>1</sup> , Junyi Yao <sup>1</sup>, Tao Wang <sup>2</sup>, Fan Wang <sup>3</sup>, Jiakuan Li <sup>1</sup>, Yuanjie Gong <sup>1</sup>, Yonggang Zhang <sup>4,\*</sup>, Jianqiu Wu <sup>4</sup>, Min Sun <sup>4</sup> and Lei Han <sup>2</sup>

<sup>1</sup> College of Civil and Architectural Engineering, Taizhou University, Taizhou 318000, China; wenxu2023@tzc.edu.cn (W.X.); junyiyao@163.com (J.Y.); lijiaxuan173783@163.com (J.L.); gongyuanjie1122@163.com (Y.G.)

<sup>2</sup> Zhejiang Construction Co., Ltd. of China Construction Eighth Engineering Division, Hangzhou 311200, China; wangtao\_zbj@163.com (T.W.); hanleiwel@163.com (L.H.)

<sup>3</sup> China Construction Third Engineering Bureau Group Co., Ltd., Wuhan 430075, China; starfanfans@hotmail.com

<sup>4</sup> Engineering Research Institute, China Construction Eighth Engineering Division Corp., Ltd., Shanghai 200122, China; jianqiuw1987@163.com (J.W.); sunmin\_6688@163.com (M.S.)

\* Correspondence: demonzhangyg@163.com

**Abstract:** Fiber-reinforced cement matrix composites (CMCs) have gained significant attention due to their ability to enhance material properties for use in demanding environments. This study investigated the workability and mechanical properties of polyvinyl alcohol (PVA) fiber-reinforced CMCs, focusing on compressive strength, split tensile strength, and flexural strength. It also assessed water absorption capacity through immersive water absorption tests using cubes and capillary water absorption tests using cylinders, alongside bulk density measurements for both shapes. The results indicated that the dosage of PVA fibers significantly influences the workability of CMCs, while the water-to-binder ratio has a minimal effect. Increasing the dosage of PVA fibers in CMCs from 0.5 vol.% to 1 vol.% led to a decrease in several properties: compressive strength decreased by 13.38%, split tensile strength by 21.05%, flexural strength by 9.23%, bulk density of cube samples by 4.14%, and bulk density of cylindrical sample by 6.36%. Conversely, both immersive water absorption and capillary water absorption increased, rising by 10.87% and 77.71%, respectively. Compressive strength was found to increase with the bulk density of the cubes and to decrease with rising immersive water absorption. Similarly, split tensile strength increased with the bulk density of the cylinders and decreased as capillary water absorption increased. Strong correlations were observed among three key pairwise combinations: the bulk density of cubes and immersive water absorption ( $R^2 = 94\%$ ), compressive strength and bulk density of cubes ( $R^2 = 96\%$ ), and compressive strength and immersive water absorption ( $R^2 = 92\%$ ). Furthermore, the analysis and comparison of carbon fiber-reinforced and PVA fiber-reinforced CMCs will provide important references for the field, especially in cases where material availability or cost varies.

**Keywords:** cement matrix composites (CMCs); mechanical property; water absorption; PVA fiber



**Citation:** Xu, W.; Yao, J.; Wang, T.; Wang, F.; Li, J.; Gong, Y.; Zhang, Y.; Wu, J.; Sun, M.; Han, L. Study on the Correlation Between Mechanical Properties, Water Absorption, and Bulk Density of PVA Fiber-Reinforced Cement Matrix Composites. *Buildings* **2024**, *14*, 3580. <https://doi.org/10.3390/buildings14113580>

Academic Editor: Mauro Mitsuchi Tashima

Received: 29 August 2024

Revised: 1 November 2024

Accepted: 8 November 2024

Published: 11 November 2024



**Copyright:** © 2024 by the authors. Licensee MDPI, Basel, Switzerland. This article is an open access article distributed under the terms and conditions of the Creative Commons Attribution (CC BY) license (<https://creativecommons.org/licenses/by/4.0/>).

## 1. Introduction

Since the end of the 20th century, research on the application of composites in cement, mortar, and concrete has attracted worldwide interest, especially in the civil engineering and construction industry, due to their enhanced material properties [1,2]. Several types of fibers, e.g., glass fiber [3], carbon fiber [4], asbestos fiber [5], polypropylene (PP) fiber [6], PVA fiber [7], or steel fiber [8], have been added to cement as reinforcing materials for improving the material properties. These CMCs can be applied to special environments according to the variety of properties of composites [9]. Therefore, significant progress has

been made in such research over the last decade. In the early 1930s, PVA fiber was first manufactured by Wacker Chemie AG Company. Over the past 90 years, the performance of PVA fiber has achieved a high level [10]. PVA fiber has become a good choice for a new generation of high-tech, environmentally friendly building materials due to its high strength, good acid-base resistance, high modulus, crack resistance, and binding with cement [11–14]. Meanwhile, its non-toxic, pollution-free, benign properties made it a favored target for more researchers [15]. Wang et al. [16] found that the introduction of PVA fiber slightly reduced the compressive strength (CS) of rubber concrete, but significantly increased the fracture energy of plain concrete. Si et al. [17] selected three types of PVA fibers as reinforcement materials for cement mortar and investigated the effects of two fiber factors on the rheological and mechanical properties of PVA fiber-reinforced CMCs. And their research revealed that when the fiber factor exceeded a certain threshold, the rheological performance of the composites significantly deteriorated. Additionally, the CS became more sensitive to matrix defects, while the flexural strength (FS) consistently increased with higher PVA fiber content. PVA fiber also positively affected the thermal conductivity, shrinkage, and crack resistance of CMCs [18]. The corrosion resistance of PVA fiber-reinforced CMCs also received good feedback [19]. PVA fibers were also added to CMCs and applied during 3D printing [20–22]. Liu et al. [23] demonstrated that adding PVA fibers to magnesium phosphate cement significantly improved its tensile strain, exceeding 3%, and increased compressive strength to 25.63 MPa within 6 h. Shen et al. [24] highlighted that while PVA fibers in ECC melt at high temperatures, they contribute to significant strength retention and performance enhancement before reaching melting point, making them crucial for maintaining mechanical integrity under elevated temperatures. Zhou et al. [25] demonstrated that modifying PVA fibers with nano-silica significantly enhances their interface properties in ultra-high-performance concrete (UHPC), leading to a 10% increase in compressive strength and over 26% flexural strength. Liu et al. [26] found that the optimal PVA fiber content for 3D printing concrete is 0.5 wt%, achieving a compressive strength of 98.2 MPa and flexural strength of 6.8 MPa. The study also highlighted significant anisotropy in the mechanical properties and acoustics of 3D-printed specimens.

There is a consensus that adding a moderate amount of PVA fibers into CMCs can perform better than traditional cementitious materials without reinforcement [27]. However, PVA fibers are usually stacked in bundles, which may lead to poor dispersion in the cement matrix, especially when added in a large amount. At the same time, uneven dispersion may weaken the properties of CMCs [28].

Török et al.'s findings on the sealing characteristics of mortar structures showed that porous materials can suffer considerable damage during freeze–thaw cycles, adversely affecting the durability of both mortars and porous materials [29]. Gruszczyński et al.'s research on the sealing characteristics of mortar structures demonstrated that the addition of silica fume and amorphous aluminum silicate, due to their small grain size, effectively filled the pores in the mortar, enhancing its structure [30]. Consequently, compared to the control mortar, water absorption decreased, and after 25 freeze–thaw cycles, the strength loss was two to three times smaller than that of the control mortar. Moore et al. [31] found that both water absorption and porosity values are crucial when evaluating the potential durability of concrete. An increase in either water absorption or porosity, or in both, leads to a decrease in the concrete's potential durability. Identifying the relationships and correlations between the mechanical properties, water absorption characteristics, and density of cement-based materials is crucial for assessing their strength. Understanding how these factors influence specific properties, such as porosity and potential durability, is particularly significant. However, research in this area remains limited. The study by Baud et al. [32] explores the effects of porosity and fracture density on the compressive strength of rocks but does not consider aspects such as water absorption. Conversely, Zhang et al. [33] concluded that there is no significant relationship between the water adsorption of concrete materials and their compressive strength. Nevertheless, they noted that surface

water absorption can predict certain concrete properties, including compressive strength and permeability. Additionally, Ramli et al. [34] found that water absorption increases with permeability, while compressive strength decreases as intrinsic permeability increases. They established a linear relationship between intrinsic permeability and the compressive strength of cement mortar, linking these findings to the influence of the pore structure of the cement paste on both water absorption and permeability. Medeiros Junior et al. [35] demonstrated that, for concrete with varying pozzolan contents, compressive strength is inversely proportional to the water-to-cement ratio, while both immersive water absorption and capillary water absorption are directly proportional to this ratio. The test results show a strong correlation among these variables. Othman et al. [36] indicated that for foam concrete, density has a strong correlation with compressive strength, with an  $R^2$  value approaching 1. However, no similar studies have been found regarding the relationship between density and mechanical properties in PVA fiber-reinforced cementitious materials.

Therefore, it is essential to investigate the relationship and correlation between the mechanical properties, water absorption, and density of PVA fiber-reinforced cementitious materials. This study aims to examine the effects of different dosages of PVA fibers by volume ( $V_f$ ) and water-to-binder ( $w/b$ ) ratios on these properties of CMCs. Additionally, exploring correlations among parameters such as compressive strength, split tensile strength, flexural strength, immersive water absorption, capillary water absorption, and bulk density of CMCs will provide a more effective evaluation of the relationship between mechanical performance and durability. Furthermore, by comparing these results with those of carbon fiber-reinforced CMCs, this study will offer valuable insights for the field, particularly regarding variations in material availability and cost.

## 2. Methodology, Materials, and Proportion Design

### 2.1. Methodology

This study focused on the mechanical properties, water absorption, and bulk density of PVA fiber-reinforced cement-based composites. The compressive strength (CS), split tensile strength (STS), and flexural strength (FS) tests followed ASTM C109 [37], ASTM 496 [38], and ASTM C78 [39], respectively.

This study carried out immersive water absorption (IWA) and capillary water absorption (CWA) tests according to ASTM C642 [40] and ASTM C1585 [41], respectively. Figures 1 and 2 show the schematics of the IWA and CWA test setups, respectively. In the IWA test, the entire sample is immersed in water, with water absorption primarily influenced by permeable pores. This test is conducted in accordance with ASTM C642. When measuring the saturated mass after immersion, the sample should be submerged in water at standard room temperature for at least 48 h, continuing until two successive mass measurements of the surface-dried sample, taken 24 h apart, show an increase of less than 0.5% of the larger value. In the CWA test, only the bottom of the cylindrical sample is immersed in water, following the guidelines of ASTM C1585. After 24 h, the increase in mass due to water ingress, which is primarily driven by the suction of the capillary pores, is measured.

In building materials, the ratio of mass to volume is known as density. Depending on the structural state, it can be categorized into true density, apparent density, and bulk density. Various definitions of density are used across different fields. In this study, we focus on bulk density, defined as the ratio of the mass of the dried sample to the volume of its external contour. This volume encompasses the surface pores, internal voids, and overall porosity of the sample. To investigate the correlations between the CS, IWA, and bulk density of cubic specimens (D-cu), as well as the correlations between the STS, CWA, and bulk density of cylindrical specimens (D-cy), we will collect the bulk densities of both cubic and cylindrical specimens.

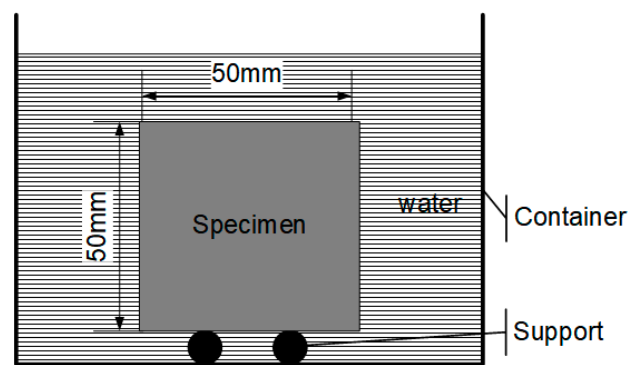


Figure 1. The schematic of the IWA test.

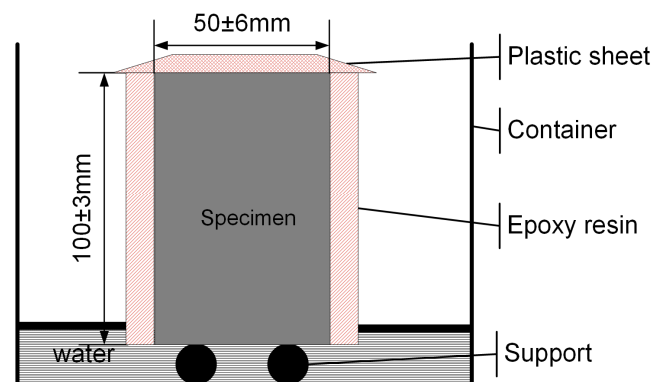


Figure 2. The schematic of the CWA test.

## 2.2. Materials

Materials used in this study, i.e., cement, lime powder, sand, water, and polycarboxylate-based superplasticizer (SP), were the same as those used in previous research [42]. PVA fibers (Qingdao Sdgeo Material Co., Ltd., Qingdao, China) illustrated in Figure 3 were selected as reinforced material for CMCs. The specifications and performance of the PVA fibers are listed in Table 1.



Figure 3. PVA fibers used in the CMCs.

Table 1. Parameters of PVA fibers.

Length	Filament	Density	Elongation	Tensile Strength	Appearance
6 mm	18 $\mu\text{m}$	1.29 g/cm <sup>3</sup>	$\leq 40\%$	1.62 GPa	White



As shown in Table 1, the density of the PVA fibers is  $1.29 \text{ g/cm}^3$ , which is lighter than that of  $1.76 \text{ g/cm}^3$  of carbon fibers used in previous research [42]. The aim of this study was not only to analyze the effect of various dosages of PVA fibers on the properties of CMCs but also to compare the effects of different fibers on CMCs (e.g., PVA and carbon fibers). Due to the differing densities of PVA fibers and carbon fibers, the comparative analysis is more meaningful when the fibers are added at the same volume fraction (relative to the total volume of CMCs without fibers). The design and calculation of the amount of PVA fibers added to the CMCs will be explained in the next section.

### 2.3. Component Proportions

In this study, six mixtures were prepared and organized into two sets, featuring two PVA fiber dosages and three water-to-binder ( $w/b$ ) ratios, to produce samples for mechanical, water absorption and bulk density tests, as illustrated in Figure 4. The two experimental sets included PVA fibers at 0.5 vol.% and 1 vol.% (relative to the total volume of CMCs designed without fibers), matching the carbon fiber amounts used in a previous study [42]. Each fiber-free mixture has a volume of  $4800 \text{ cm}^3$ . The binder materials, a 9:1 ratio of cement to lime powder, have a content of  $700 \text{ kg/m}^3$ . The SP dosage was based on the dosage recommendations provided by the supplier (Sika® ViscoCrete®-2100, Lyndhurst in New Jersey, USA), with proportions relative to the binder materials in the six mixtures being 16, 19, 22, 19, 22, and 16, respectively. The density of the SP is  $1.08 \text{ g/mL}$  [42], while the density of PVA fibers is  $1.29 \text{ g/cm}^3$ . According to the calculation results, the masses of cement (C), lime powder (LP), water (W), sand (S), superplasticizer (SP), and PVA fiber (F) in each mixture are detailed in Table 2.

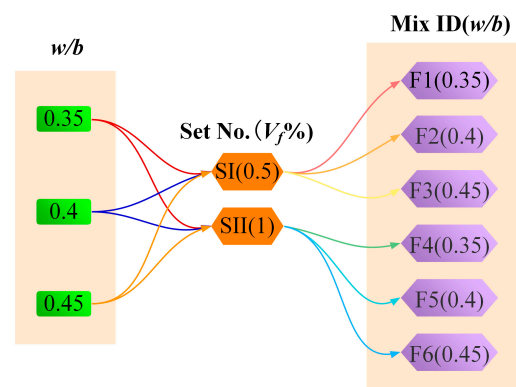


Figure 4. Six mixtures designed in this study.

Table 2. Component amount of the six mixtures.

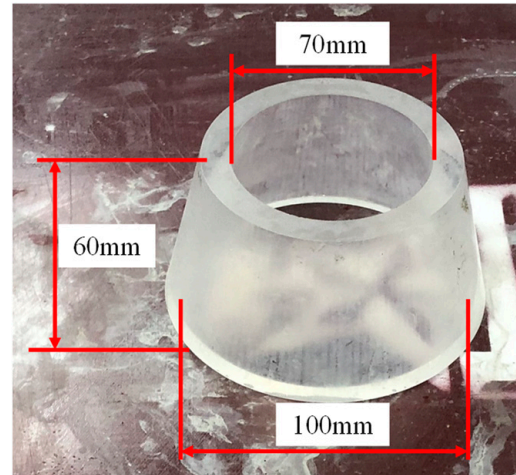
Set No. ( $V_f\%$ )	Mix ID ( $w/b$ )	Component (kg)					
		Cement	Lime Powder	Water	Sand	SP	Fiber
SI (0.5 vol.%)	F1 (0.35)	3.0240	0.3360	1.1760	6.0240	0.0575	0.0310
	F2 (0.4)	3.0240	0.3360	1.3440	5.8560	0.0683	0.0310
	F3 (0.45)	3.0240	0.3360	1.5120	5.6880	0.0791	0.0310
SII (1 vol.%)	F4 (0.35)	3.0240	0.3360	1.1760	6.0240	0.0683	0.0619
	F5 (0.4)	3.0240	0.3360	1.3440	5.8560	0.0791	0.0619
	F6 (0.45)	3.0240	0.3360	1.5120	5.6880	0.0575	0.0619

### 2.4. Mixing Procedures and Sample Preparation

The preparations of dry materials, i.e., cement, lime powder, fine aggregates, PVA fibers, and solution (i.e., water and SP), were carried out after the amount of the ingredients was determined and calculated. Both needed to be pre-mixed. First, the dry materials were mixed in a dry state for one minute. Then, while continuing the mixing, the solution was

added to the mixer to mix with the dry materials. The mixing continued for 2 min, followed by 30 s of manual mixing. Finally, another 3 min of machine mixing was performed.

After preparing the fresh mixtures, workability tests were immediately conducted on the fresh CMCs using the mini slump cone shown in Figure 5.




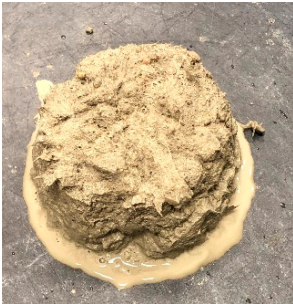




**Figure 5.** Mini slump cone for workability tests.

Testing method for mini slump: a mini slump cone with an upper diameter of 70 mm, a lower diameter of 100 mm, and a height of 60 mm is filled with the fresh mixture. After filling, a tamper is used to evenly tamp the cone from the outside to the inside for 10 strokes, followed by leveling the surface. The cone is then removed, allowing the mixture to slump under its own weight. The mini slump is defined as the height of the cone (60 mm) minus the height of the mixture after slumping. For example, if the difference is 2 mm, then the mini slump is 2.

The results of the workability tests for the six mixtures, along with fresh mixture images, are presented in Table 3. The experimental results indicate that PVA fibers have a significant impact on workability of CMCs. Under the same  $w/b$  ratio, the mini slump of SI (0.5 vol.%) is greater than that of SII (1 vol.%) by 0.99–1.1 mm. When comparing within the SI (F1, F2, F3) at the same PVA fiber dosage, it is observed that as the  $w/b$  ratio increases from 0.35 to 0.45, the mini slump only increases by 0.3 mm. For the SII (F4, F5, F6), under the same increment of the  $w/b$  ratio, the mini slump increases by just 0.4 mm. These results indicate that the flowability of the PVA fiber-reinforced CMCs is relatively weak, with the  $w/b$  ratio having minimal impact on flowability, while the PVA fiber dosage has a significant influence.

While conducting workability tests on the fresh CMCs, specimens for CS, FS, STS, IWA, and CWA tests were also prepared. Cube samples measuring  $50 \times 50 \times 50$  mm were prepared for the CS and IWA tests, while cylindrical samples with a diameter of 50 mm and a height of 100 mm were prepared for the STS and CWA tests. Additionally, beam samples measuring  $25 \times 25 \times 285$  mm were prepared for the FS test. The fresh mortar was immediately placed into the cube, cylinder, and beam molds after mixing. Following this, the molds were gently tapped, and the mortar surface was smoothed with a scraper. The molds were then covered with plastic sheets and left at room temperature. After 24 h, the samples were demolded and moved to a curing room maintained at 20 °C and 95% relative humidity. The mechanical properties, water absorption, and bulk density tests were conducted after 28 days of curing.

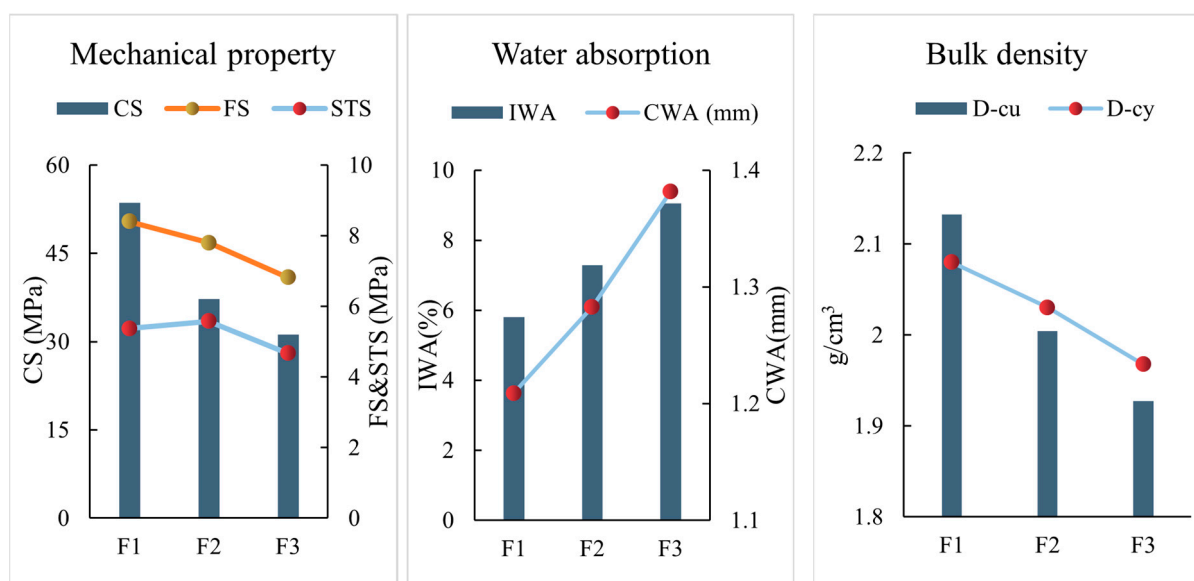
**Table 3.** Workability tests result of the six mixtures.

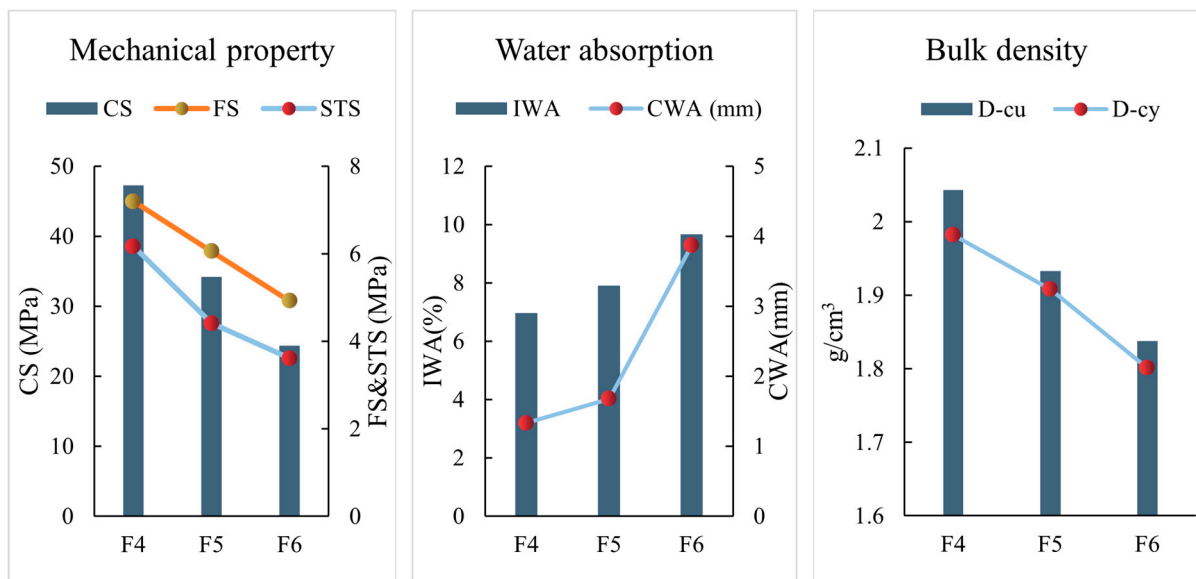
Set No.	Mix ID—Mini Slump and Fresh Mixture Image		
SI	F1—Mini Slump (1.2)	F2—Mini Slump (1.4)	F3—Mini Slump (1.5)
			
	F4—Mini Slump (0.2)	F5—Mini Slump (0.3)	F6—Mini Slump (0.6)
SII			

### 3. Results and Analysis

#### 3.1. Test Results Under Different $w/b$ Ratios

The CS, STS, FS, IWA, and CWA tests were performed on the PVA fiber-reinforced CMCs samples after a 28-day curing period. To compare the effects of different  $w/b$  ratios on mechanical property, water absorption, and bulk density of CMCs with the same PVA fiber dosage, the experimental results of SI ( $V_f = 0.5$  vol.%) and SII ( $V_f = 1$  vol.%) are shown in Figures 6 and 7, respectively.

**Figure 6.** The comparison results of SI ( $V_f = 0.5$  vol.%).



**Figure 7.** The comparison results of SII ( $V_f = 1$  vol.%).

Figure 6 illustrates that, for a constant dosage of PVA fibers ( $V_f = 0.5$  vol.%), increasing the  $w/b$  ratio—specifically, F1(0.35), F2(0.4), and F3(0.45)—resulted in decreases in CS, FS, STS, as well as the bulk density of both the cube samples (D-cu) and the cylindrical sample (D-cy) by 41.72%, 18.92%, 13.04%, 9.64%, and 5.40%, respectively. Conversely, IWA and CWA increased by 55.67% and 14.29%, respectively. Figure 7 shows that, for a constant dosage of PVA fibers ( $V_f = 1$  vol.%), increasing the  $w/b$  ratio—specifically, F4(0.35), F5(0.4), and F6(0.45)—resulted in decreases in CS, FS, STS, D-cu, and D-cy by 48.48%, 31.58%, 41.52%, 10.03%, and 9.10%, respectively. In contrast, IWA and CWA increased by 38.84% and a significant 190.74%, respectively. This occurs because, as the  $w/b$  ratio increases, the water content also rises. After cement hydration, excess water remains in CMCs. When this moisture evaporates, it creates voids, leading to a decrease in the bulk density of the specimens and an increase in water absorption. Additionally, the presence of irregular voids reduces the effective cross-sectional area of the CMCs that bears loads. Under loading conditions, this can result in stress concentration around the voids, ultimately decreasing strength. Xin et al. [43] observed that, with a consistent amount of PVA fibers, both the FS and tensile strength of PVA-engineered cementitious composites increased gradually as the  $w/b$  ratio decreased. In contrast, Chung et al. [44] noted that, in line with established principles regarding concrete materials, the CS of engineering cementitious composites is inversely related to the  $w/b$  ratio. Additionally, Medeiros Junior et al. [35] studied the performance of concrete with varying volcanic ash content, revealing that the CS is inversely proportional to the water-to-cement ratio. It is worth noting that, as the  $w/b$  ratio increases, the CS, FS, and STS of CMCs with 1 vol.% PVA fiber decreases more significantly than that of CMCs with 0.5 vol.% PVA fiber. This demonstrated that for the same material and the same volume, the smaller the bulk density, the more pores contained in the sample, and the larger the porosity of the sample, which was also confirmed by the experimental results of IWA and CWA.

### 3.2. Impact on the Test Results Under Different $V_f$

In this study, the subjects were divided into two sets based on different dosages of PVA fibers, as illustrated in Figure 4, with each set consisting of three different water-to-binder ratios. In this section, we averaged the experimental results for the three  $w/b$  within each set, concentrating specifically on the effects of varying fiber dosages on the performance of the CMCs. The CS, FS, STS, D-cu, IWA, D-cy, and CWA of CMCs with 0.5 vol.% and 1 vol.% PVA fiber dosages are presented in Table 4. It was observed that CS,



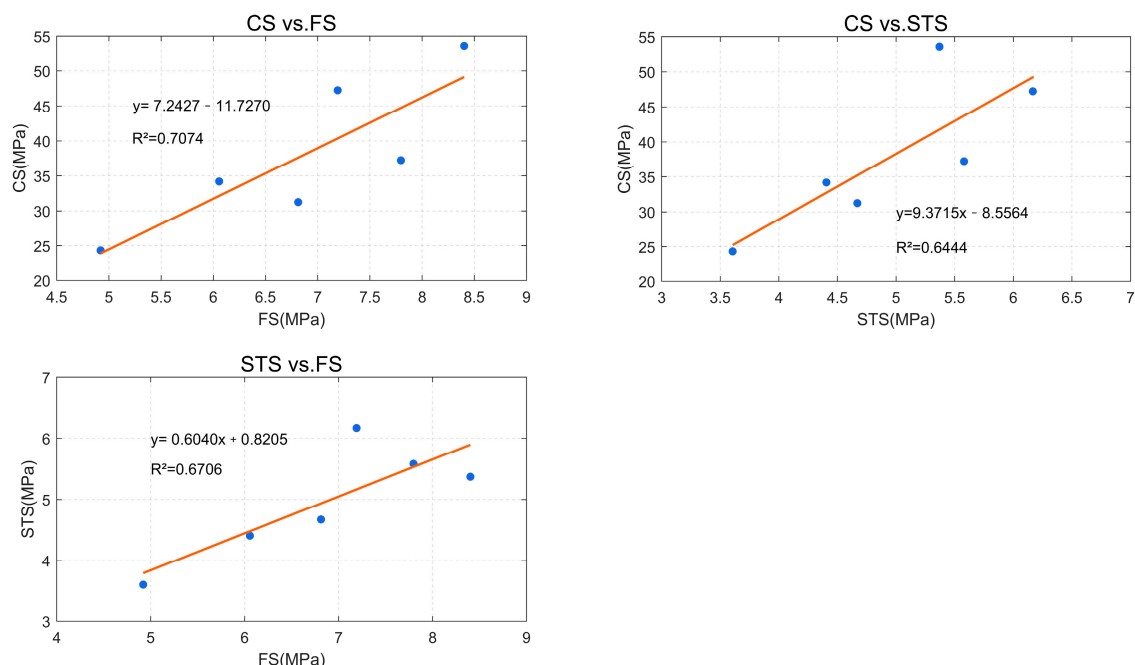
FS, STS, D-cu, and D-cy decreased with increasing PVA fiber dosage, showing declines of 13.38%, 21.05%, 9.23%, 4.14%, and 6.36%, respectively. In contrast, IWA and CWA increased by 10.87% and 77.71%, respectively. The strength of CMCs did not improve with an increase in fiber dosage when the PVA fiber content was raised from 0.5 vol.% to 1 vol.%. Similar findings have been reported by other researchers [16,45,46]. Wang et al. [16] found that the incorporation of PVA fibers slightly reduced the CS of rubberized concrete. Shen et al. [45] explained that higher dosages of PVA fibers can lead to a looser gel pore structure and decalcification of calcium silicate hydrate gels, particularly in cementitious composites with high volumes of fly ash. This results in increased capillary porosity and a corresponding reduction in strength and durability. Yao et al. [46] observed that excessive PVA fiber content caused entanglement, adversely affecting CS in concrete. These studies indicate that as the amount of PVA fibers increases, the CS of various types of cement-based materials is negatively impacted.

**Table 4.** CS, FS, STS, D-cu, IWA, D-cy, and CWA under different  $V_f$ .

Set No.	$V_f$ (%)	CS (MPa)	FS (MPa)	STS (MPa)	D-cu (g/cm <sup>3</sup> )	IWA (%)	D-cy (g/cm <sup>3</sup> )	CWA (mm)
SI	0.50	40.71	7.67	5.21	2.02	7.38	2.03	1.29
SII	1.00	35.26	6.06	4.73	1.94	8.18	1.90	2.29

### 3.3. Correlation Analysis Between Response Values

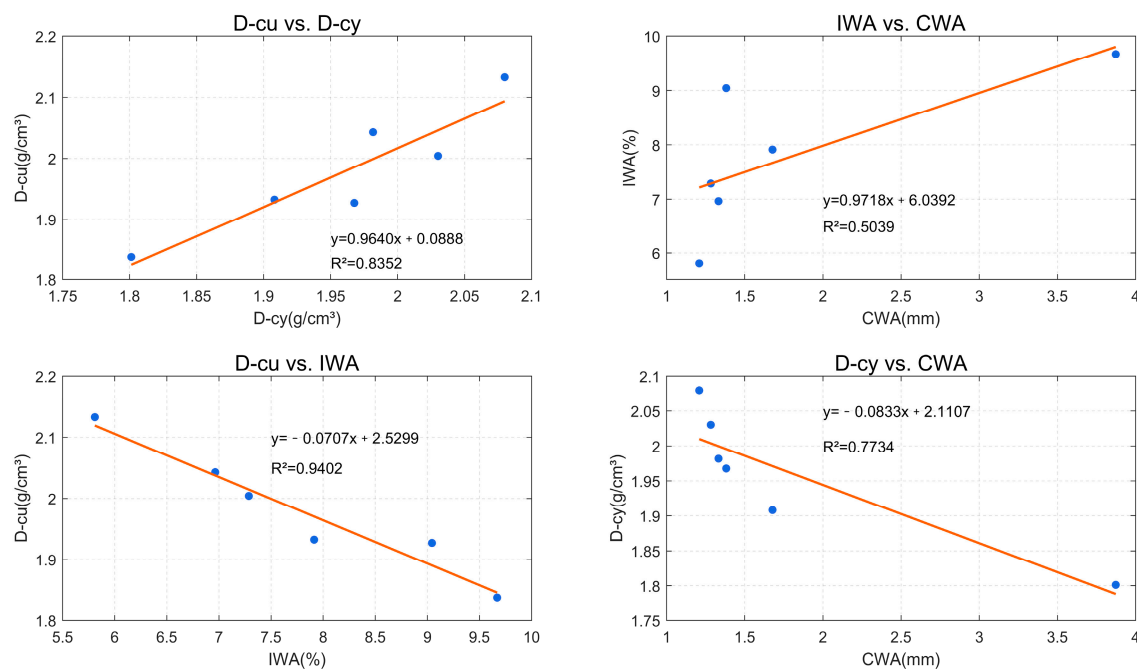
The previous analysis demonstrated that with the increase in  $w/b$  ratio and  $V_f$ , the mechanical properties and density of CMCs decreased while the water absorption increased. The correlations analysis was performed to analyze the correlations between these responses. The correlations between CS, FS, and STS are shown in Figure 8. The correlations between CS, FS, and STS are so weak that it was challenging to obtain another value from one of them in this work.



**Figure 8.** The correlations of CS vs. FS, CS vs. STS, and STS vs. FS.

The correlations between IWA, CWA, D-cu, and D-cy are illustrated in Figure 9. It was observed that there is a strong correlation between D-cu and IWA, with the regression equation given by  $y = -0.07073x + 2.530$  and an  $R^2$  value of 0.94. In contrast, the correlation between D-cy and CWA is relatively low, with an  $R^2$  of 0.734.





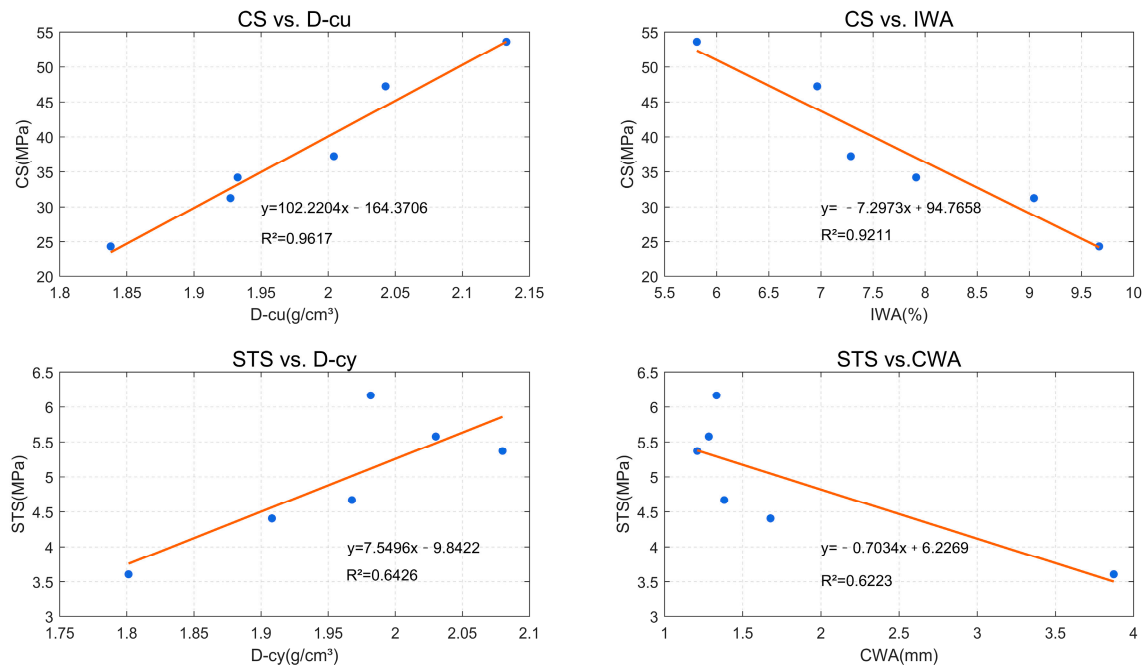
**Figure 9.** The correlations of D-cu vs. D-cy, IWA vs. CWA, D-cu vs. IWA, and D-cy vs. CWA.

It is important to note that the IWA and CWA tests were conducted using cubic and cylindrical specimens, respectively, while D-cu and D-cy represent the bulk densities of these specimens. This difference in test setups may explain the observed results. In the IWA test, the amount of water absorbed is primarily influenced by the permeable voids in the cubic samples, whereas in the CWA test, water absorption is driven by the capillary pores in the cylindrical samples. A decrease in bulk density indicates an increase in porosity, with permeable voids playing a more significant role in this context.

Consequently, the cubic specimens in the IWA test absorbed more water, while the cylindrical specimens in the CWA test absorbed less. As a result, there is a more pronounced negative correlation between D-cu and IWA, while the negative correlation between D-cy and CWA is less evident.

This study utilized cube samples for CS, IWA, and D-cu tests. Cylindrical samples were employed for STS, CWA and D-cy tests. Beam specimens were employed for FS test, but not designed for water absorption and bulk density tests; therefore, the correlations between FS and water absorption and bulk density were not analyzed. The correlations among four pairwise combinations—specifically, CS and D-cu, CS and IWA, STS and D-cy, and STS and CWA—are illustrated in Figure 10. The analysis revealed that the correlations between CS and D-cu, and between CS and IWA, with  $R^2$  values of 96% and 92%, respectively, are significantly stronger than those between STS and D-cy and between STS and CWA, which have  $R^2$  values of 64% and 62%, respectively. Additionally, Figure 10 indicates that, regardless of the  $R^2$  values of the correlations, both CS and STS increase with rising bulk density and decrease with increasing water absorption capacity. Currently, there is limited research on the correlations between parameters (CS, IWA, D-cu) and (STS, CWA, D-cy) in the study of the performance of PVA fiber-reinforced CMCs. However, studies on other cementitious materials suggest similar interrelationships among these parameters, even without linear fitting. For instance, Ramli et al. [34] found that in their research on polymer-modified cement mortars, CS decreases while IWA increases with higher permeability. This indicates that, in these cement composites, as water absorption increases, CS decreases. Similarly, Medeiros Junior et al. [35] examined the performance of concrete with varying volcanic ash content and discovered that CS is inversely proportional to the water-to-cement ratio, while the IWA is directly proportional to the same ratio. This further supports the idea that, in this type of concrete, CS decreases as IWA increases.

Kim et al. [47] also reported that in their study of ordinary and high-strength mortars, CS decreases and water absorption increases with an increase in the  $w/b$  ratio. Thus, for both types of mortars, there is an inverse relationship between CS and water absorption. Overall, the literature indicates a consistent inverse relationship between CS and water absorption in cement-based materials. This paper has conducted linear fitting on these two parameters, and further research is anticipated, either in future studies or by other scholars, to confirm correlations with additional parameters such as density and STS.



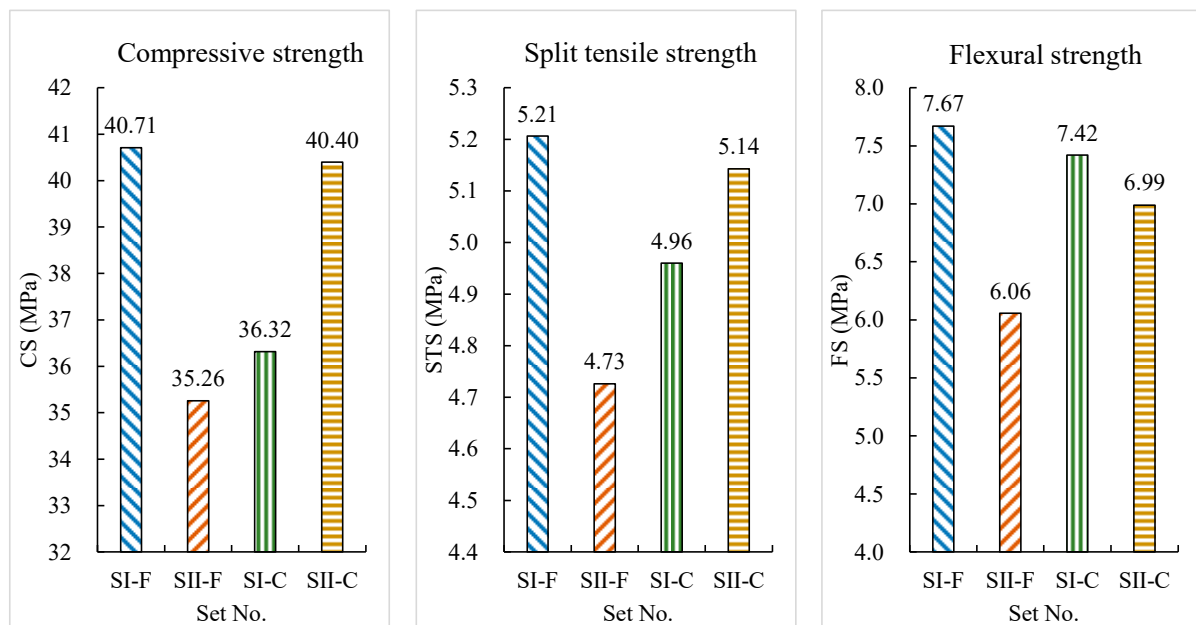
**Figure 10.** The correlations of CS vs. D-cu, CS vs. IWA, STS vs. D-cy, and STS vs. CWA.

#### 4. Influence of Carbon and PVA Fibers on CMCs

Previous studies investigated the mechanical properties and water absorption of carbon fiber-reinforced CMCs with varying volume fractions (0.5 vol.% and 1 vol.%) [42]. To offer a more comprehensive reference for selecting fiber materials for cement-based composites, the effects of carbon and PVA fibers on the properties of CMCs are compared and analyzed as follows.

##### 4.1. Effect of Fiber Type on Mechanical Properties of CMCs

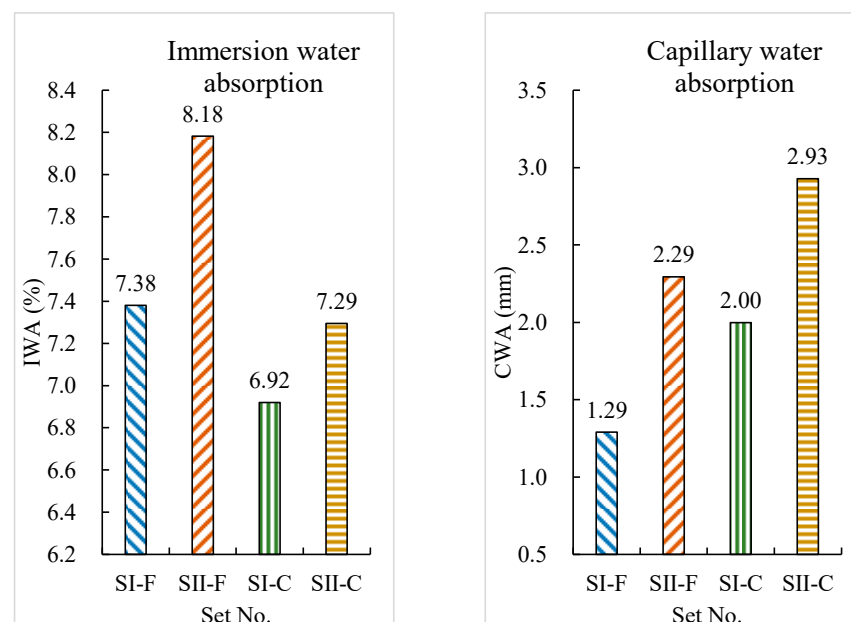
The CS, STS, and FS of PVA fiber-reinforced CMCs (SI-F and SII-F) and carbon fiber-reinforced CMCs (SI-C and SII-C) with varying fiber dosages (SI: 0.5 vol.%, SII: 1 vol.%) are shown in Figure 11. Figure 11 illustrates that the CS, STS, and FS all decrease as the content of PVA fibers increases, with reductions of 13.38%, 9.23%, and 21.05%, respectively. In contrast, both CS and STS increase with higher carbon fiber content, showing increases of 11.24% and 3.68%, respectively. However, FS decreases with increasing carbon fiber content, with a reduction of 5.78%.



**Figure 11.** Mechanical properties of CMCs with varying fiber dosages.

#### 4.2. Effect of Fiber Type on Water Absorption Properties of CMCs

The results of the IWA and CWA tests for both PVA fiber-reinforced CMCs (SI-F and SII-F) and carbon fiber-reinforced CMCs (SI-C and SII-C) with varying fiber dosages (SI: 0.5 vol.%, SII: 1 vol.%) are presented in Figure 12. It was observed that both IWA and CWA increased with the dosage of PVA and carbon fibers, indicating that higher amounts of both fiber types resulted in an increased water absorption (pore content) in the CMCs.



**Figure 12.** Water absorption capacity of CMCs with varying fiber dosages.

#### 4.3. Brief Summary

By comparing Figure 11 with Figure 12, it can be observed that, when the dosage of PVA fibers increases, the water absorption of PVA fiber-reinforced CMCs increases (indicating an increase in porosity), while the CS and STS of the PVA fiber-reinforced CMC decline. However, with the increase in carbon fiber dosage, the water absorption

of carbon fiber-reinforced CMCs also increases, but both the CS and STS of the carbon fiber-reinforced CMCs improve. This suggests that the CS and STS can still be enhanced despite the increased porosity of the cube and cylindrical specimens with higher carbon fiber content. This improvement may be attributed to the superior bonding between carbon fiber filaments and the cementitious matrix in CMCs. Further investigation is necessary to understand how these two types of fiber filaments bond with the cementitious matrix and how these micro-mechanisms influence the mechanical properties of CMCs.

It was confirmed that 0.5 vol.% PVA fibers and 1 vol.% carbon fibers had an equivalent effect on the CS, STS and water absorption capacity of CMCs. In practice, reasonable selection can be made according to the specific special environment and the economic benefits of PVA and carbon fibers.

## 5. Conclusions

The primary aim of this study was to investigate the effects of PVA fiber content and *w/b* ratio on the mechanical properties, water absorption, bulk density, and their correlation in CMCs. Additionally, this study analyzed and compared the performance differences between PVA fiber-reinforced CMCs and carbon fiber-reinforced CMCs across various fiber contents. The key findings are as follows:

- (1) The workability of CMCs declines as the PVA fiber content increases and the water-to-binder ratio decreases. However, workability is primarily influenced by the amount of PVA fibers, while the effect of the water-to-binder ratio is comparatively minor.
- (2) Increasing the dosage of PVA fibers from 0.5 vol.% to 1 vol.% resulted in decreases in CS, STS, FS, D-cu, and D-cy by 13.38%, 21.05%, 9.23%, 4.14%, and 6.36%, respectively. Conversely, IWA and CWA increased by 10.87% and 77.71%, respectively.
- (3) For the PVA fiber-reinforced CMCs, strong correlations were observed among three pairwise combinations—specifically, D-cu and IWA, CS and D-cu, and CS and IWA—with  $R^2$  values of 94%, 96%, and 92%, respectively. Meanwhile, moderate correlations were found among three others pairwise combinations—specifically, D-cy and CWA, STS and D-cy, and STS and CWA—with  $R^2$  values of 77%, 64%, and 62%, respectively. Both CS and STS increase with increasing bulk density and decrease with increasing water absorption capacity.
- (4) The CS and STS of CMCs reinforced with 0.5 vol.% PVA fibers—40.71 MPa and 5.21 MPa, respectively—were comparable to those of CMCs reinforced with 1 vol.% carbon fibers—40.40 MPa and 5.14 MPa, respectively.

**Author Contributions:** Conceptualization, W.X., J.Y., T.W. and Y.Z.; Data curation, W.X., F.W. and M.S.; Formal analysis, J.L. and J.W.; Funding acquisition, W.X. and Y.Z.; Investigation, J.Y., Y.G. and Y.Z.; Methodology, W.X., T.W. and Y.Z.; Project administration, W.X., Y.Z. and M.S.; Resources, W.X. and Y.Z.; Supervision, W.X., Y.Z. and L.H.; Validation, W.X., J.Y., F.W., J.W. and L.H.; Visualization, T.W., F.W. and J.L.; Writing—original draft, W.X., J.L. and Y.G.; Writing—review and editing, W.X., J.Y. and Y.G. All authors have read and agreed to the published version of the manuscript.

**Funding:** This research was funded by the Industrial Science and Technology Program of Taizhou S&T Bureau (no. 23gyb15) and the 2024 National College Student Innovation and Entrepreneurship Training Program of Taizhou University (no. 2024103500038).

**Data Availability Statement:** The original contributions presented in the study are included in the article, further inquiries can be directed to the corresponding author.

**Conflicts of Interest:** Authors Tao Wang and Lei Han were employed by the company Zhejiang Construction Co., Ltd. of China Construction Eighth Engineering Division. Author Fan Wang was employed by the company China Construction Third Engineering Bureau Group Co., Ltd. Authors Yonggang Zhang, Jianqiu Wu and Min Sun were employed by the Engineering Research Institute, China Construction Eighth Engineering Division Corp., Ltd. The remaining authors declare that the research was conducted in the absence of any commercial or financial relationships that could be construed as a potential conflict of interest.

## References

1. Manso-Morato, J.; Hurtado-Alonso, N.; Revilla-Cuesta, V.; Skaf, M.; Ortega-Lopez, V. Fiber reinforced concrete and its life cycle assessment: A systematic review. *J. Build. Eng.* **2024**, *94*, 110062. [\[CrossRef\]](#)
2. Gu, L.; Liu, Y.; Zeng, J.; Zhang, Z.; Pham, P.N.; Liu, C.; Zhuge, Y. The synergistic effects of fibres on mechanical properties of recycled aggregate concrete: A comprehensive review. *Constr. Build. Mater.* **2024**, *436*, 137011. [\[CrossRef\]](#)
3. Jiang, Y.; Xu, J.; Yu, Z.; Liu, L.; Chu, H. Improving conductivity and self-sensing properties of magnetically aligned electroless nickel coated glass fiber cement. *Cem. Concr. Compos.* **2023**, *137*, 104929. [\[CrossRef\]](#)
4. Tao, Y.; Liu, J.; Zhang, D.; Xie, Z.; Hong, J. Effect of iccp on bond performance and piezoresistive effect of carbon fiber bundles in cementitious matrix. *Cem. Concr. Compos.* **2024**, *152*, 121943. [\[CrossRef\]](#)
5. Ranaivomanana, H.; Leklou, N. Investigation of microstructural and mechanical properties of partially hydrated asbestos-free fiber cement waste (afcc) based concretes: Experimental study and predictive modeling. *Constr. Build. Mater.* **2021**, *277*, 121943. [\[CrossRef\]](#)
6. Shen, D.; Liu, C.; Luo, Y.; Shao, H.; Zhou, X.; Bai, S. Early-age autogenous shrinkage, tensile creep, and restrained cracking behavior of ultra-high-performance concrete incorporating polypropylene fibers. *Cem. Concr. Compos.* **2023**, *138*, 104948. [\[CrossRef\]](#)
7. Zhang, X.; Wang, B.; Ju, Y.; Wang, D.; Zhu, M. Experimental study and new model for flexural parameters of steel-pva high-performance fiber reinforced concrete. *J. Mater. Civ. Eng.* **2023**, *35*, 04023073. [\[CrossRef\]](#)
8. Yoo, D.-Y.; Soleimani-Dashtaki, S.; Oh, T.; Chun, B.; Choi, J.-S.; Banthia, N.; Yoon, Y.S. Effects of amount and geometrical properties of steel fiber on shear behavior of high-strength concrete beams without shear reinforcement. *Cem. Concr. Compos.* **2024**, *151*, 105606. [\[CrossRef\]](#)
9. Li, J.; Xia, J.; Di Sarno, L.; Gong, G. Fiber utilization in pervious concrete: Review on manufacture and properties. *Constr. Build. Mater.* **2023**, *406*, 133372. [\[CrossRef\]](#)
10. Yao, S.; Hu, C.; Wang, F.; Hu, S. Improving the interfacial properties of pva fiber and cementitious composite: Design and characterization. *Constr. Build. Mater.* **2023**, *409*, 134163. [\[CrossRef\]](#)
11. Yang, Y.; Chen, B.; Chen, Y.; Liu, F.; Xie, X.; Guo, W.; Wang, H. Effect of admixtures and pva fiber on the mechanical properties of high strength cementitious grout. *Case Stud. Constr. Mater.* **2023**, *18*, e01884. [\[CrossRef\]](#)
12. Abbas, Y.M.; Hussain, L.A.; Khan, M.I. Constitutive compressive stress-strain behavior of hybrid steel-pva high-performance fiber reinforced concrete. *J. Mater. Civ. Eng.* **2022**, *34*, 04021401. [\[CrossRef\]](#)
13. Guan, Y.; Li, Y.; Zhang, H.; Sun, R.; Tian, J.; Yang, Y. Preparation of low-cost green engineered cementitious composites (ecc) using gold tailings and uncoiled pva fiber. *J. Build. Eng.* **2023**, *78*, 107455. [\[CrossRef\]](#)
14. Zang, Y.; Sun, M.; Hou, D.; Wang, X.; Wang, M.; Zhao, T.; Xu, R.; Wang, P. Assessing interfacial bonding performance of pva fiber and cement hydration products: An atomic simulation. *J. Mater. Civ. Eng.* **2021**, *36*, 04023596. [\[CrossRef\]](#)
15. Wang, H.; Xu, J.; Song, Y.; Hou, M.; Xu, Y. Development of low-cost engineered cementitious composites using yellow river silt and uncoiled pva fiber. *Constr. Build. Mater.* **2024**, *425*, 136063. [\[CrossRef\]](#)
16. Wang, J.; Dai, Q.; Si, R.; Guo, S. Investigation of properties and performances of Polyvinyl Alcohol (PVA) fiber reinforced rubber concrete. *Constr. Build. Mater.* **2018**, *193*, 631–642. [\[CrossRef\]](#)
17. Si, W.; Cao, M.; Li, L. Establishment of fiber factor for rheological and mechanical performance of polyvinyl alcohol (PVA) fiber reinforced mortar. *Constr. Build. Mater.* **2020**, *265*, 120347. [\[CrossRef\]](#)
18. Wang, F.; Yang, Y.; Yin, S. Thermal and moisture performance parameters of high toughness engineered cementitious composite(ecc) with pva fibers. *J. Build. Eng.* **2021**, *43*, 102905. [\[CrossRef\]](#)
19. Chen, Z.; Zhao, G.; Wei, J.; Chen, C.; Tang, Y. Residual impact resistance behavior of pva fiber reinforced cement mortar containing nano-sio2 after exposure to chloride erosion. *Constr. Build. Mater.* **2024**, *414*, 134990. [\[CrossRef\]](#)
20. Luo, S.; Li, W.; Wang, D. Study on bending performance of 3d printed pva fiber reinforced cement-based material. *Constr. Build. Mater.* **2024**, *433*, 136637. [\[CrossRef\]](#)
21. Wang, L.; Hu, Y.; Wang, Q.; Cui, T. Shrinkage and cracking performance of pp/pva fiber reinforced 3d-printed mortar. *J. Mater. Civ. Eng.* **2023**, *35*, 04023132. [\[CrossRef\]](#)
22. Ziada, M.; Tanyildizi, H.; Seloglu, M.; Coskun, A. Bacteria-based crack healing of 3d printed pva fiber reinforced geopolymer mortars. *J. Build. Eng.* **2024**, *86*, 108934. [\[CrossRef\]](#)
23. Liu, J.; Yan, C.; Liu, S.; Jing, L.; Yin, L.; Wang, X. Toughness and strength of pva-fibre reinforced magnesium phosphate cement (frmpc) within 24 h. *Constr. Build. Mater.* **2024**, *418*, 135339. [\[CrossRef\]](#)
24. Shen, S.; Zhuang, J.; Yang, Y.; Dong, S. Mechanical performances and micro-level properties of basalt and pva fiber reinforced engineered cementitious composite after high temperatures exposure. *J. Build. Eng.* **2023**, *79*, 107870. [\[CrossRef\]](#)
25. Zhou, Y.; Huang, J.; Yang, X.; Dong, Y.; Feng, T.; Liu, J. Enhancing the pva fiber-matrix interface properties in ultra high performance concrete: An experimental and molecular dynamics study. *Constr. Build. Mater.* **2021**, *285*, 122862. [\[CrossRef\]](#)
26. Liu, B.; Liu, X.; Li, G.; Geng, S.; Li, Z.; Weng, Y.; Qian, K. Study on anisotropy of 3d printing pva fiber reinforced concrete using destructive and non-destructive testing methods. *Case Stud. Constr. Mater.* **2022**, *17*, e01519. [\[CrossRef\]](#)
27. Mousavinejad, S.H.G.; Alemi, M.P. Micro-structural and mechanical properties of pva fiber reinforced engineered cementitious composite incorporating natural and artificial pozzolanic materials under different temperatures. *Constr. Build. Mater.* **2022**, *346*, 128180. [\[CrossRef\]](#)



28. Lu, C.; Yuan, Z.; Yang, C.; Hou, D.; Yao, Y. Tensile properties of pva and pe fiber reinforced engineered cementitious composites containing coarse silica sand. *J. Build. Eng.* **2023**, *75*, 106913. [[CrossRef](#)]
29. Török, Á.; Szemerey-Kiss, B. Freeze-thaw durability of repair mortar sand porous limestone: Compatibility issues. *Prog. Earth Planet. Sci.* **2019**, *6*, 42. [[CrossRef](#)]
30. Gruszczyński, M.; Lenart, M. Durability of mortars modified with the addition of amorphous aluminum silicate and silica fume. *Theor. Appl. Fract. Mech.* **2020**, *107*, 102526. [[CrossRef](#)]
31. Moore, A.J.; Bakera, A.T.; Alexander, M.G. A critical review of the Water Sorptivity Index (WSI) parameter for potential durability assessment: Can WSI be considered in isolation of porosity? *J. South Afr. Inst. Civ. Eng.* **2021**, *63*, 27–34. [[CrossRef](#)]
32. Baud, P.; Wong, T.F.; Zhu, W. Effects of porosity and crack density on the compressive strength of rocks. *Int. J. Rock Mech. Min. Sci.* **2014**, *67*, 202–211. [[CrossRef](#)]
33. Zhang, S.P.; Zong, L. Evaluation of relationship between water absorption and durability of concrete materials. *Adv. Mater. Sci. Eng.* **2014**, *2014*, 1–8. [[CrossRef](#)]
34. Ramli, M.; Tabassi, A.A. Effects of polymer modification on the permeability of cement mortars under different curing conditions: A correlational study that includes pore distributions, water absorption and compressive strength. *Constr. Build. Mater.* **2012**, *28*, 561–570. [[CrossRef](#)]
35. Junior, R.A.M.; Munhoz, G.S.; Medeiros, M.H.F. Correlations between water absorption, electrical resistivity and compressive strength of concrete with different contents of pozzolan. *Rev. Alconpat* **2019**, *9*, 152–166. [[CrossRef](#)]
36. Othman, R.; Jaya, R.P.; Muthusamy, K.; Sulaiman, M.; Duraisamy, Y. Relation between density and compressive strength of foamed concrete. *Materials* **2021**, *14*, 2967. [[CrossRef](#)]
37. ASTM C109 2020; Standard Test Method for Compressive Strength of Hydraulic Cement Mortars. ASTM International: West Conshohocken, PA, USA, 2020; pp. 1–11.
38. ASTM C496 2017; Standard Test Method for Splitting Tensile Strength of Cylindrical Concrete Specimens. ASTM International: West Conshohocken, PA, USA, 2017; pp. 1–5.
39. ASTM C78 2018; Standard Test Method for Flexural Strength of Concrete (Using Simple Beam with Third-Point Loading). ASTM International: West Conshohocken, PA, USA, 2018; pp. 1–5.
40. ASTM C642 2013; Standard Test Method for Density, Absorption, and Voids in Hardened Concrete. ASTM International: West Conshohocken, PA, USA, 2013; pp. 1–3.
41. ASTM C1585 2013; Standard Test Method for Measurement of Rate of Absorption of Water by Hydraulic-Cement Concretes. ASTM International: West Conshohocken, PA, USA, 2013; pp. 1–6.
42. Xu, W.; Jalal, M.; Zakira, U.; Wang, L.J.I.C.S.E.; Science, E. Study on the mechanical properties and durability of carbon fiber reinforced lime-based mortar. *IOP Conf. Ser. Earth Environ. Sci.* **2021**, *719*, 032032. [[CrossRef](#)]
43. Xin, Q.; Gao, R.; Lv, W.; Wei, H. Effect of Different Water-Binder Ratios and Fiber Contents on the Fluidity and Mechanical Properties of PVA-ECC Materials. *Teh. Vjesn.* **2023**, *30*, 1366–1372. [[CrossRef](#)]
44. Chung, K.L.; Ghannam, M.; Zhang, C. Effect of specimen shapes on compressive strength of engineered cementitious composites (ECCs) with different values of water-to-binder ratio and PVA fiber. *Arab. J. Sci. Eng.* **2018**, *43*, 1825–1837. [[CrossRef](#)]
45. Shen, Y.; Li, Q.; Huang, B.; Liu, X.; Xu, S. Effects of pva fibers on microstructures and hydration products of cementitious composites with and without fly ash. *Constr. Build. Mater.* **2022**, *360*, 129533. [[CrossRef](#)]
46. Yao, J.; Ge, Y.; Ruan, W.; Meng, J. Effects of pva fiber on shrinkage deformation and mechanical properties of ultra-high performance concrete. *Constr. Build. Mater.* **2024**, *417*, 135399. [[CrossRef](#)]
47. Kim, H.K.; Jeon, J.H.; Lee, H.K. Flow, water absorption, and mechanical characteristics of normal-and high-strength mortar incorporating fine bottom ash aggregates. *Constr. Build. Mater.* **2012**, *26*, 249–256. [[CrossRef](#)]

**Disclaimer/Publisher’s Note:** The statements, opinions and data contained in all publications are solely those of the individual author(s) and contributor(s) and not of MDPI and/or the editor(s). MDPI and/or the editor(s) disclaim responsibility for any injury to people or property resulting from any ideas, methods, instructions or products referred to in the content.